

Electromagnetic Interaction in the System of Multimonopoles and Vortex Rings

Yasha Shnir

Institut für Physik, Universität Oldenburg, D-26111, Oldenburg, Germany

Behavior of static axially symmetric monopole-antimonopole and vortex ring solutions of the $SU(2)$ Yang-Mills-Higgs theory in an external uniform magnetic field is considered. It is argued that the axially symmetric monopole-antimonopole chains and vortex rings can be treated as a bounded electromagnetic system of the magnetic charges and the electric current rings. The magnitude of the external field is a parameter which may be used to test the structure of the static potential of the effective electromagnetic interaction between the monopoles with opposite orientation in the group space. It is shown that for a non-BPS solutions there is a local minimum of this potential.

PACS numbers: 14.80.Hv,11.15Kc

I. INTRODUCTION

The structure of the vacuum of the $SU(2)$ Yang-Mills-Higgs (YMH) theory is rather nontrivial (see. e.g., [1, 2]), there are spherically symmetric monopoles with unit topological charge [3], axially symmetrical multimonopoles of higher topological charge [4, 5, 6], and solutions with platonic symmetry [1, 7]. There is also a monopole-antimonopole (M-A) pair static solution, which is a deformation of the topologically trivial sector [8, 9]. Recently, another deformations of this sector, which represented monopole-antimonopole chains and vortex rings, were discussed [10]. There are also electrically charged generalizations of these solutions [11, 12, 13], which appear due to excitation of the gauge zero modes of the underlying electrically neutral solutions.

These solutions are characterized by two integers, the winding number m in polar angle θ and the winding number n in azimuthal angle φ . The structure of the nodes of the Higgs field depends on the values of these integers, there are both chains of zeros and rings. However, only the winding number n has a meaning of the topological charge of the configuration.

In the Bogomol'nyi-Prasad-Sommerfield (BPS) limit of vanishing Higgs potential the spherically symmetric monopole and axially symmetric multimonopole solutions, which satisfy the first order Bogomol'nyi equations [14] as well as the second order field equations, are known analytically [6].

Taubes proved that in the $SU(2)$ YMH theory a smooth, finite energy magnetic dipole solution of the second order field equations, which do not satisfy the Bogomol'nyi equations, could exist [16]. In his consideration the space of the field configurations and the energy functional are considered as the manifold and the function, respectively. For a monopole-antimonopole pair (M-A) the map $S^2 \rightarrow S^2$ has a degree zero, thus it is a deformation of the topologically trivial sector. A generator for the corresponding homotopy group is a non-contractible loop which describes creation of a monopole-antimonopole pair with relative orientation in the isospace $\delta = -\pi$ from the vacuum, separation of the pair, rotation of the monopole by 2π and annihilation of the pair back into vacuum. Minimization of the energy functional along such a loop yields an equilibrium state in the middle of the loop where the monopole is rotated by π and $\delta = 0$. Such an axially symmetric configuration, with two zeros of the Higgs field located symmetrically on the positive and negative z -axis, corresponds to a saddlepoint of the energy functional, a monopole and antimonopole in static equilibrium, a magnetic dipole [8, 9].

It is interesting to compare the situation with the case of two monopoles. It was shown long ago [17], that there is a balance of two long-range interactions between the BPS monopoles, which are mediated by the massless photon and the massless scalar particle, respectively. The balance of interactions, which yields the magnetic dipole solution, is a bit more subtle. Indeed, a monopole and an antimonopole can only be in static equilibrium, if they are close enough to experience a repulsive force [9, 10] which may balance the electromagnetic and scalar attractions. In this case we have a complicated pattern of short-range interactions and the structure of the nodes of the Higgs fields strongly depends on the scalar coupling [10]. All these Yukawa interactions result in an effective potential of interaction whose local minimum corresponds, for example, to the static dipole solution.

Evidently, an external electromagnetic field may be used as a "dipstick" to test the structure of the net potential of the interaction between the poles. In this note I argue that one can make use of an effective electromagnetic interaction in such solutions, which encompasses the complicated picture of the short-range Yukawa forces above. Further, to support this interpretation, I study the interaction of different static axially symmetric deformations of the topologically trivial sector, both monopoles and vortex rings, with an external uniform magnetic field.

In section II we present the action, the axially symmetric Ansatz and the boundary conditions. In section III we discuss the effect of coupling of the system with an external homogeneous magnetic field and consider the behavior

of the forced monopole-antimonopole pairs and vortex rings. We present our conclusions in section IV.

II. YANG-MILLS-HIGGS SOLUTIONS: MONOPOLE-ANTIMONOPOLE CHAINS AND VORTEX RINGS

The Lagrangian of the Yang-Mills-Higgs model is given by

$$-L_0 = \int \left\{ \frac{1}{2} \text{Tr} (F_{\mu\nu} F^{\mu\nu}) + \frac{1}{4} \text{Tr} (D_\mu \Phi D^\mu \Phi) + \frac{\lambda}{8} \text{Tr} [(\Phi^2 - \eta^2)^2] \right\} d^3 r , \quad (1)$$

with $su(2)$ gauge potential $A_\mu = A_\mu^a \tau^a / 2$, field strength tensor $F_{\mu\nu} = \partial_\mu A_\nu - \partial_\nu A_\mu + ie[A_\mu, A_\nu]$, and covariant derivative of the Higgs field $\Phi = \phi^a \tau^a$ in the adjoint representation $D_\mu \Phi = \partial_\mu \Phi + ie[A_\mu, \Phi]$. Here e denotes the gauge coupling constant, η the vacuum expectation value of the Higgs field and λ the strength of the Higgs selfcoupling.

The static regular solutions of the corresponding field equations were constructed numerically by employing of the axially symmetric Ansatz [10] for the gauge and the Higgs fields

$$\begin{aligned} A_\mu dx^\mu &= \left(\frac{K_1}{r} dr + (1 - K_2) d\theta \right) \frac{\tau_\varphi^{(n)}}{2e} - n \sin \theta \left(K_3 \frac{\tau_r^{(n,m)}}{2e} + (1 - K_4) \frac{\tau_\theta^{(n,m)}}{2e} \right) d\varphi \\ \Phi &= \Phi_1 \tau_r^{(n,m)} + \Phi_2 \tau_\theta^{(n,m)} . \end{aligned} \quad (2)$$

The Ansatz is written in the basis of $su(2)$ matrices $\tau_r^{(n,m)}, \tau_\theta^{(n,m)}$ and $\tau_\varphi^{(n)}$ which are defined as the dot product of the Cartesian vector of Pauli matrices $\vec{\tau}$ and the spacial unit vectors

$$\begin{aligned} \hat{e}_r^{(n,m)} &= (\sin(m\theta) \cos(n\varphi), \sin(m\theta) \sin(n\varphi), \cos(m\theta)) , \\ \hat{e}_\theta^{(n,m)} &= (\cos(m\theta) \cos(n\varphi), \cos(m\theta) \sin(n\varphi), -\sin(m\theta)) , \\ \hat{e}_\varphi^{(n)} &= (-\sin(n\varphi), \cos(n\varphi), 0) , \end{aligned} \quad (3)$$

respectively. The gauge field functions $K_i, i = 1, \dots, 4$ and two Higgs field functions Φ_1, Φ_2 depend on the coordinates r and θ . The axial symmetry of the configuration allows also to consider the system in cylindrical coordinates with the planar radius $\rho = r \sin \theta$.

The Ansatz (2) is axially symmetric in a sense that a spacial rotation around the z -axis can be compensated by Abelian gauge transformation $U = \exp\{i\omega(r, \theta)\tau_\varphi^{(n)}/2\}$ which leaves the Ansatz form-invariant. However the gauge potential and the scalar field transform as

$$A'_\mu = U A_\mu U^\dagger + \frac{i}{e} (\partial_\mu U) U^\dagger, \quad \Phi' = U \Phi U^\dagger$$

respectively. Then the structure functions of the Ansatz transforming as [9]

$$\begin{aligned} K_1 &\rightarrow K_1 - r \partial_r \omega; \quad K_2 \rightarrow K_2 + \partial_\theta \omega; \\ \left(K_3 + \frac{\cos(m\theta)}{\sin \theta} \right) &\rightarrow \left(K_3 + \frac{\cos(m\theta)}{\sin \theta} \right) \cos \omega + \left(1 - K_4 - \frac{\sin(m\theta)}{\sin \theta} \right) \sin \omega; \\ \left(1 - K_4 - \frac{\sin(m\theta)}{\sin \theta} \right) &\rightarrow - \left(K_3 + \frac{\cos(m\theta)}{\sin \theta} \right) \sin \omega + \left(1 - K_4 - \frac{\sin(m\theta)}{\sin \theta} \right) \cos \omega; \\ \Phi_1 &\rightarrow \Phi_1 \cos \omega + \Phi_2 \sin \omega; \quad \Phi_2 \rightarrow -\Phi_1 \sin \omega + \Phi_2 \cos \omega . \end{aligned} \quad (4)$$

To obtain a regular solution we make use of the $U(1)$ gauge symmetry to fix the gauge [15]. We impose the condition

$$G_f = \frac{1}{r^2} (r \partial_r K_1 - \partial_\theta K_2) = 0 .$$

The regular solutions with finite energy density and correct asymptotic behavior are constructed numerically by imposing the boundary conditions. The regularity of the energy density functional at the origin requires

$$K_1(0, \theta) = 0, \quad K_2(0, \theta) = 1, \quad K_3(0, \theta) = 0, \quad K_4(0, \theta) = 1 ,$$

$$\sin(k\theta)\Phi_1(0, \theta) + \cos(k\theta)\Phi_2(0, \theta) = 0 ,$$

$$\partial_r [\cos(k\theta)\Phi_1(r,\theta) - \sin(k\theta)\Phi_2(r,\theta)]|_{r=0} = 0$$

that is $\Phi_\rho(0,\theta) = 0$ and $\partial_r\Phi_z(0,\theta) = 0$.

Since here we are discussing only the topologically trivial sector of the model, the related configurations at infinity required to tend to a pure gauge

$$\Phi \longrightarrow U\tau_z U^\dagger, \quad A_\mu \longrightarrow i\partial_\mu UU^\dagger, \quad (5)$$

where $U = \exp\{-ik\theta\tau_\varphi^{(n)}\}$ and $m = 2k$. Therefore in terms of the functions $K_1 - K_4$, Φ_1 , Φ_2 these boundary conditions read [26]

$$K_1 \longrightarrow 0, \quad K_2 \longrightarrow 1 - 2k, \quad K_3 \longrightarrow 0, \quad K_4 \longrightarrow 1 - \frac{2\sin(k\theta)}{\sin\theta}, \quad (6)$$

$$\Phi_1 \longrightarrow \cos(k\theta), \quad \Phi_2 \longrightarrow \sin(k\theta). \quad (7)$$

Regularity on the z -axis, finally, requires

$$K_1 = K_3 = \Phi_2 = 0, \quad \partial_\theta K_2 = \partial_\theta K_4 = \partial_\theta \Phi_1 = 0,$$

for $\theta = 0$ and $\theta = \pi$.

Thus, the deformations of the topologically trivial sector are classified according to the values of the winding numbers k and n . The branch of solutions with $k = 1$ corresponds to the monopole-antimonopole pair M-A ($n = 1$) [9], the charge-2 monopole-antimonopole pair ($n = 2$) [10, 21] and a single vortex ring ($n \geq 3$). Another branch with $k = 2$ corresponds to the monopole-antimonopole chain M-A-M-A with 4 nodes of the Higgs field on the z -axis ($n = 1$), chain of 4 double nodes ($n = 2$) and the system of two vortex rings ($n \geq 3$) [9]. The energy of these configurations increases with n .

The axially symmetric solutions under consideration are characterised by a non-vanishing magnetic dipole moment [9, 10]. It can be read off from the asymptotic form of the gauge field at infinity

$$A_\mu dx^\mu = \mu \frac{\sin^2\theta}{2r} \tau_z d\varphi, \quad (8)$$

where μ is a (dimensionless) magnetic dipole moment.

Note that the pattern of interaction between the monopoles is very different from a naive picture of electromagnetic interaction of point-like charges [1, 2, 17]. Indeed, there is such an attractive force between well separated monopole and antimonopole, in the singular gauge, it is mediated by the A^3 component of the vector field. However, this field is massless only outside of the monopole core. On the other hand, it is known that the BPS monopoles do not interact at any separation which allows us to make use of the powerful moduli space approach (see, e.g., [1]). The reason is that the repulsive vector interaction between the poles is always balanced by the scalar interaction.

However, the axially symmetric configurations which we are discussing, are not solutions of the first order Bogomol'nyi equation, even in the limit of vanishing scalar coupling where scalar interaction also becomes long-range. They are deformation of the topologically trivial sector and, on the scale of characteristic size of the axially symmetric solutions, both the scalar particle and the A_μ^3 vector boson remain massive. Furthermore, the vector bosons A_μ^\pm also mediate the short-range Yukawa interactions between the monopoles and we have to take into account all these contributions.

Taubes pointed out [16] that the latter contribution to the net potential depends on the relative orientation of the monopoles in the group space which is parametrised by an angle δ . Magnetic dipole solution above corresponds to the saddle point configuration where the attractive short-range forces, mediated both by the A_μ^3 vector boson and the Higgs boson, are balanced by the repulsive interaction. The latter forces are mediated by the massive vector bosons A_μ^\pm with opposite orientation in the group space. There is a difference from a system of two identically charged BPS monopoles where the scalar attraction is cancelled due to contribution of the repulsive gauge interaction. Note that the boundary conditions on the fields at the spatial asymptotic (5) above, for example for M-A pair $k = 1$, yield the rotation of the fields on the negative semi-axis z by π , with respect to the fields on the positive semi-axis z . Evidently, this corresponds to the Taubes conjecture for a magnetic dipole.

III. ELECTROMAGNETIC PROPERTIES OF THE CONFIGURATIONS

A. Effective electromagnetic interaction

Thus, the pattern of interaction between the monopoles is very different from a naive picture of Coulomb long-range electromagnetic interaction of point-like charges. It looks a bit surprising, but there is also a possibility to describe this system in terms of an effective electromagnetic interaction associated with the regular Abelian electromagnetic field strength tensor

$$\mathcal{F}_{\mu\nu} = \text{Tr} \left\{ \hat{\Phi} F_{\mu\nu} - \frac{i}{2e} \hat{\Phi} D_\mu \hat{\Phi} D_\nu \hat{\Phi} \right\}. \quad (9)$$

Here we make use of the normalization $\hat{\Phi} = \Phi/\eta$. Thus, in a regular gauge all the components of the vector field are projected there onto direction of the Higgs field and corresponding excitation, a photon, is massive inside of the monopole core.

This gauge-invariant definition of the electromagnetic field strength tensor $F_{\mu\nu}$, given in [22], is close to the original definition of the 't Hooft tensor [3], up to replacement $\hat{\Phi}$ with a normalized Higgs field $\Phi/|\Phi|$. Obviously, both definitions coincide on the spacial boundary. The difference is that the 't Hooft tensor is singular at the zeros of the Higgs field, while (9) is regular everywhere. In both cases the zeros are associated with positions of the monopoles.

Note that the definition of an electromagnetic field strength tensor is always somewhat arbitrary in a non-Abelian gauge theory, for example one can also consider $\mathcal{F}_{\mu\nu} = \hat{\phi}^a F_{\mu\nu}^a$ [22, 23].

Let us briefly recapitulate the electromagnetic properties of the solutions [10]. The electromagnetic field strength tensor (9) yields both the electric current j_{el}^ν

$$\partial_\mu \mathcal{F}^{\mu\nu} = 4\pi j_{\text{el}}^\nu, \quad (10)$$

and the magnetic current j_{mag}^ν

$$\partial_\mu {}^* \mathcal{F}^{\mu\nu} = 4\pi j_{\text{mag}}^\nu. \quad (11)$$

The magnetic charge of the configuration is defined as

$$g = \frac{1}{4\pi\eta} \int \frac{1}{2} \text{Tr} (F_{ij} D_k \Phi) \varepsilon_{ijk} d^3 r. \quad (12)$$

In the topologically trivial sector it vanishes, however the charge density distribution $g(x) = \frac{1}{2} \text{Tr} (F_{ij} D_k \Phi) \varepsilon_{ijk}$ is not trivial. Evidently, the electric current j_{el}^ν is vanishing for the spherically symmetric 't Hooft–Polyakov solution.

As mentioned above, the axially symmetric configurations possess a magnetic dipole moment which, in such an effective electromagnetic framework, can be evaluated from the magnetic charge density and the electric current density as [24],

$$\vec{\mu} = (\mu_{\text{charge}} + \mu_{\text{current}}) \vec{e}_z = \int \left(\vec{r} g(x) - \frac{1}{2} \vec{r} \times \vec{j}_{\text{el}} \right) d^3 r. \quad (13)$$

Results of the numerical calculations show that the estimated dipole moment μ_{est} quite agrees with the exact value μ obtained from asymptotic expansion [10] (see Table 1)

n/k	μ		μ_{est}	
	1	2	1	2
1	4.71	9.87	4.43	9.48
2	4.75	9.63	5.38	9.76
3	5.20	9.96	4.92	10.07
4	5.75	10.65	5.26	10.84

Table 1 The dipole moment μ and the estimated electromagnetic dipole moment μ_{est} are given for the solutions of the first and second branches with several values of n at $\lambda = 0$.

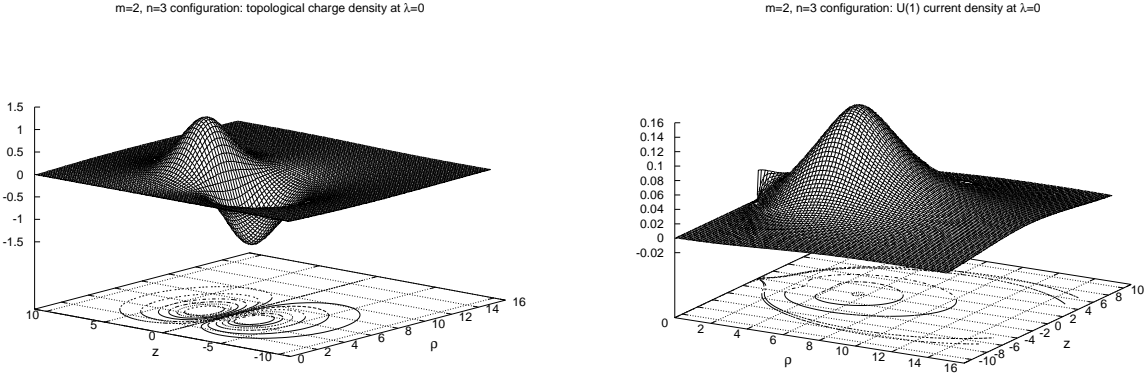


Figure 1: The charge density (left) and electric current density (right) are shown for solution with $k = 1, n = 3$ at $\lambda = 0$ as functions of the coordinates z, ρ .

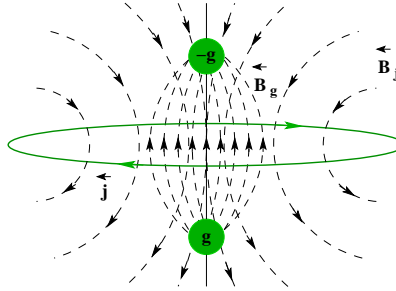


Figure 2: Electromagnetic picture of an equilibrium state of two opposite magnetic charges in the magnetic field of the electric current ring.

Thus, the physical picture of the source of the dipole moment is that it originates both from a distribution of the magnetic charges and the electric currents [10]. Because of axial symmetry of the configurations, $\vec{\mu} = \mu \vec{e}_z$.

Let us consider the charge and current density distributions given by the relations (12) and (10), respectively. We can evaluate these electromagnetic quantities by straightforward substitution of the numerical solutions with given k and n into the definitions above.

To construct solutions subject to the above boundary conditions, we map the infinite interval of the variable r onto the unit interval of the compactified radial variable $x \in [0 : 1]$,

$$x = \frac{r}{1+r} ,$$

i.e., the partial derivative with respect to the radial coordinate changes according to $\partial_r \rightarrow (1-x)^2 \partial_x$. The numerical calculations are then performed with the help of the FIDISOL package based on the Newton-Raphson iterative procedure [25]. The equations are discretized on a non-equidistant grid in x and θ with typical grids sizes of 70×60 . The estimates of the relative error for the functions are of the order of 10^{-4} . The results were presented in [9, 10].

Making use of these solutions, we can see that there is a single electric current ring for the first branch of the solutions with $k = 1$ (see Fig. 1). This current is circulating exactly between the maxima of distributions of the positive and negative charge density. For $n = 1$ the latter are located at the z axis and coincide with positions of the nodes of the Higgs field. For solution with $n = 2$ the maxima of the charge density distribution form two rings parallel to xy -plane where the current ring is placed. Also the energy density of the configuration represents two tori. However two (double) zeroes of the Higgs field still are on the z axis. The energy density tori are located symmetrically with respect to the nodes of the Higgs field.

As winding number n increases further, i.e., $n \geq 3$, instead of isolated nodes on the symmetry axis, the closed vortex solution arises [10]. For this configuration the Higgs field vanishes on a closed ring centered around the symmetry axis. This ring coincides with position of maxima of the current density distribution. Thus, one may conjecture that the

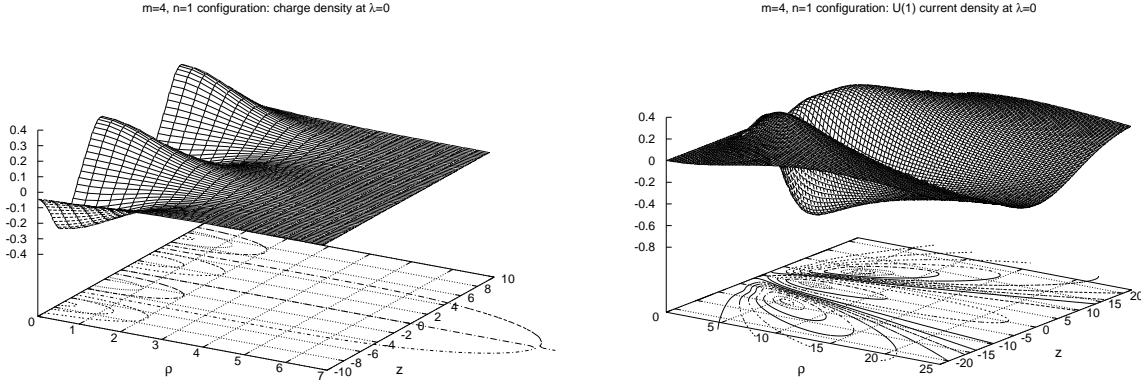


Figure 3: The magnetic charge density (left) and the electric current density (right) distributions are shown for M-A-M-A chain solution with $k = 2, n = 1$ at $\lambda = 0$ as functions of the coordinates z, ρ .

stability of the chain and vortex configurations is due to balance of the effective electromagnetic interaction between the poles and current rings. Indeed, the $U(1)$ magnetic field is generated both by the static distribution of the density of the magnetic charges, and by the circular electric current. There is the magnetic field \mathcal{B}_k of the current loop which stabilizes the configuration and counteract the attraction between two opposite charges (cf. Fig. 2).

For second branch of the solutions with $k = 2$ three current rings centered around the symmetry axis arise, one counterclockwise in the xy -plane, and two outer clockwise rings which lie in planes parallel to the xy -plane. As in the case of the first branch, these current rings are circulating between the maxima of distributions of the positive and negative charge density. The effect of the magnetic field generated by these currents is to provide a balance of electromagnetic interactions in such a system of charges and currents.

Let us consider, for example the M-A-M-A chain with $n = 1$. There are two pairs of maxima of positive and negative charge density distribution on the z axis associated with position of the nodes of the Higgs field and the radius of the inner current ring is a bit smaller than the radius of two other rings (see Fig. 3).

As winding number n is increases further, the situation is changing. The maxima of the charge density distribution of the $k = 2$ configuration with $n = 2$ are no longer coincide with double nodes of the Higgs field which still are on the z axis. They form four rings with current density tori squeezed between them. Further increasement of n leads to separation of the nodes from the symmetry axis. As n increases beyond two, the nodes move onto the ρ axis and form two vortex rings located symmetrically. The radius of the rings of nodes increases with n . Also the radius of three current loops increases, however, for the vortex configuration the radius of the inner ring is getting larger than two outer rings. The values of the corresponding parameters of all these rings depend on the scalar coupling λ . In general, for larger values of λ the radius of the rings is smaller and they are closer to the xy -plane.

B. Coupling with an external electromagnetic field: Forced axially symmetric configurations

To analyse the structure of the net potential of interaction between the poles, let us couple the configurations with an external electromagnetic field. This can be done by addition to the Lagrangian (1) a gauge invariant term

$$L_{int} = \frac{1}{2} \varepsilon_{nmk} \mathcal{F}_{mk} B_n^{ext},$$

which describes the direct electromagnetic interaction between the magnetic field of the field configuration and the external homogeneous magnetic field B_{ext} [18]. To preserve the axial symmetry of the configuration, we suppose that this field is directed along z axis, either in positive or in negative direction.

Such a field can be used as a free perturbation parameter of the model which allows to manipulate the configuration moving the nodes and transforming its structure. If the forced configuration remains static, the energy of the related quasi-elastic deformation is balanced by the energy of interaction, thus the structure of the net effective potential of the electromagnetic interaction may be revealed.

It was shown that for a single 't Hooft-Polyakov monopole inclusion of this term of interaction yields an excitation of the monopole zero modes and accelerate the monopole precisely by analogy with a motion of a point-like charge in

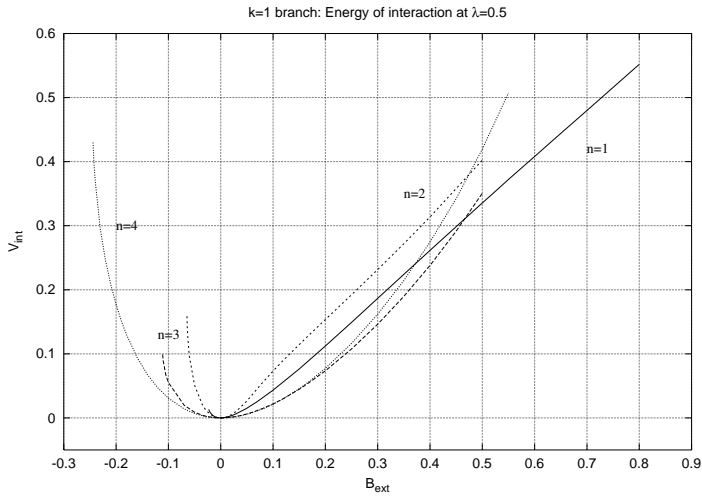


Figure 4: Energy of interaction of the static solutions of the $k = 1$ branch as a function of an external magnetic field at $\lambda = 0.5$.

an external electromagnetic field [18]. Let us consider how inclusion of such a term affects the static axially symmetric deformations of the topologically trivial sector.

The $k = 1$ branch begins from the unperturbed magnetic dipole solution $n = 1$ [8, 9] with two zeros of the Higgs field on the symmetry axis. The charge density distribution has two picks of opposite sign, located on the positive and negative z axis, respectively. They are associated with positive and negative magnetic charges of the dipole [9]. In the BPS limit the rescaled mass of configuration is $M_0 = 1.69$ and the distance between the nodes is $z_0 = 4.18$ in units of v.e.v. of the scalar field [8, 9]. As λ increases the equilibrium distance is getting smaller and for $\lambda = 0.5$ we have $z_0 = 3.24$ and $M_0 = 2.48$.

When an external interaction perturbs the configuration, the situation changes. Numerical calculations shows that if the external magnetic field is directed along negative direction of the z axis there is an additional electromagnetic attraction in the system which pushes the poles closer to each other.

We observe similar behavior both for a finite and vanishing scalar coupling λ . This case resembles the situation when gravity is coupled [19, 20]. As the magnitude of the external magnetic field B_{ext} increases, the nodes of the scalar field, which are associated with position of the poles, are approaching to each other. The potential energy V_{int} of electromagnetic interaction on that branch, which is calculated as the difference $V_{int} = E - M_0$, depends almost linearly on the external field (see Fig 4) for positive values of B_{ext} .

Evidently, this corresponds to the expectable electrodynamical picture of interaction of two pointlike opposite charges with an external homogeneous field. As the magnitude of the external field increases further, the nodes of the solution continue to approach each other. However a novelty is observed as the external field reaches some critical value, for $\lambda = 0.5$ it happens as $B_{ext} = 0.515$ and the poles merge at the origin. Here the pole and antipole do not annihilate, however. The configuration cannot annihilate into the trivial sector because of the boundary conditions which we imposed on the spacial infinity. Only the modes, that are orthogonal to the Ansatz (2) may contribute to this process.

As the magnitude of the external magnetic field B_{ext} becomes stronger, a single vortex ring appears instead of a monopole-antimonopole pair. The radius of the ring is increasing with further increase of the magnitude of the external field. However, the energy of interaction still linearly depends on the magnitude of the external field.

If the external magnetic field is directed along positive direction of the z axis, there is an additional repulsion in the system. We observed that for a finite value of scalar coupling, the potential of electromagnetic interaction develops a local minimum. Indeed, in this case with increasing the magnitude of the external magnetic field, the poles moves away from each other until some critical distance between the nodes is reached. Then the numerical errors are getting relative large and the calculation routine converges badly. Actually as $\lambda = 0.5$ for $B_{ext} \sim -0.027$ already a tiny further increase of the magnitude of perturbation results in large shift of the nodes of the scalar field (see Fig. 6 right). With increasing λ the minimum of the potential becomes sharper. Considering the solutions in the BPS limit, however, we do not find a static monopole-antimonopole pair BPS solution for any finite value of B_{ext} .

We observe a similar scenario considering configuration with $k = 1, n = 2$. Again, for a finite value of B_{ext} a branch of solutions emerges from the non-interacting solution. However, the energy of interaction between the double charged poles in that case is stronger, thus the monopole-vortex transition is observed at the smaller value of B_{ext} as in the

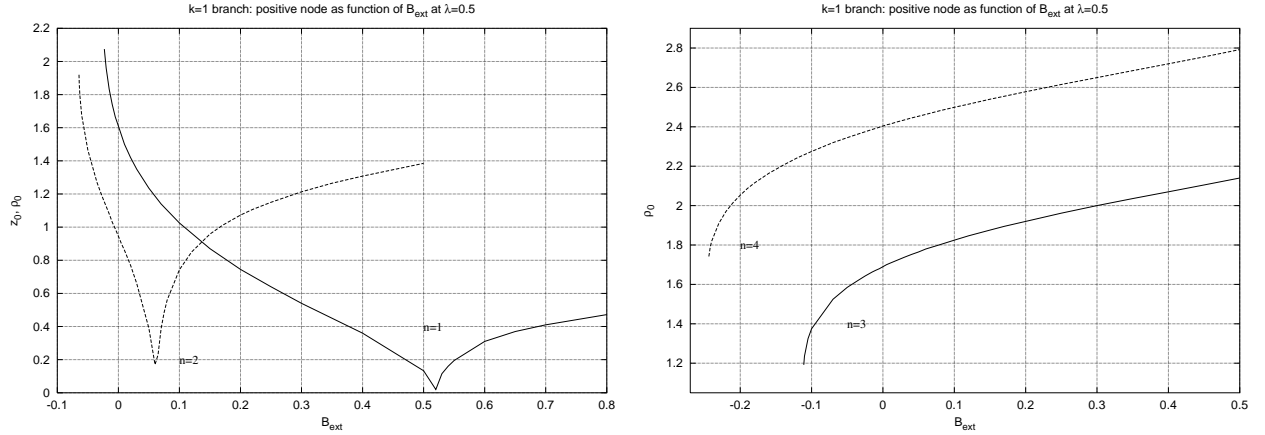


Figure 5: Position of nodes of the Higgs field of the chain solutions of the $k = 1$ branch ($n = 1, 2$ left, and $n = 3, 4$, right) as function of the external magnetic field at $\lambda = 0.5$.

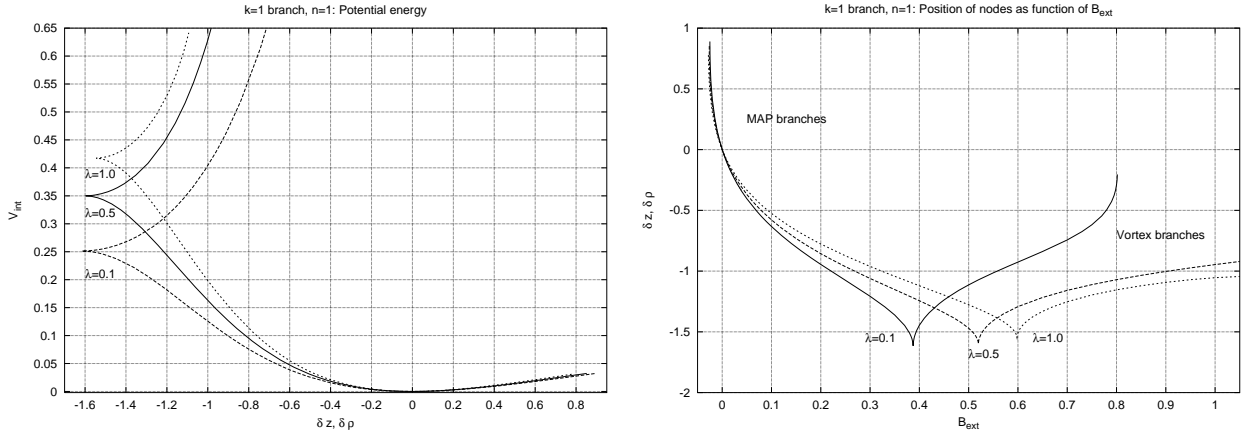


Figure 6: Potential of monopole-antimonopole interaction of the $k = 1$ branch (left) and position of the nodes as a function of B_{ext} (right) for different values of λ .

case of $k = 1, n = 1$ configuration. Furthermore, the potential well is also deeper (see Fig. 7).

Recall that the solutions with $k = 1, n \geq 3$ are no longer characterized by some discrete set of isolated poles on the symmetry axis. They are the vortex rings already, without an external interaction. The dipole moment of these configurations arises solely from the electric current (10) and the current ring appears there as a source of the magnetic field [10]. Testing the vortex solutions with external magnetic field we observe quite expectable electrodynamical picture: the radius of the current ring is increasing as the magnitude B_{ext} of the magnetic field, which is directed along positive direction of the symmetry axis, increases. In contrast, as the external field is directed in opposite direction, the vortex ring is shrinking. This branch is expended up to some critical value of B_{ext} beyond which external field becomes too strong for static configuration to persist.

Since for a static configuration the energy of interaction with an external field is equal to the potential energy of the quasi-elastic deformation, the shape of the potential energy well can be easily recovered from the consideration above, see Figs. 6,7. Evidently, there is a bifurcation which resembles a second order phase transition for the solutions of the first branch with $n = 1, 2$. This bifurcation is related with transformation of the dipole configuration into the vortex ring. With increasing λ the potential well is getting more deep.

Similar behavior under external perturbation develop also the solutions in the $k = 2$ branch. For example, $n = 1$ configuration is a chain solution M-A-M-A, which represent 2 interpolating monopole-antimonopole pairs. As magnitude of the external field increases, each of two M-A pairs evolves similar to the scenario above; relative potential of interaction almost exactly reproduces the plot presented in Figs. 6 and 7. Likewise, there is a chain-rings transition for a critical value of the external magnetic field, each pair forms a vortex ring those radius is increasing

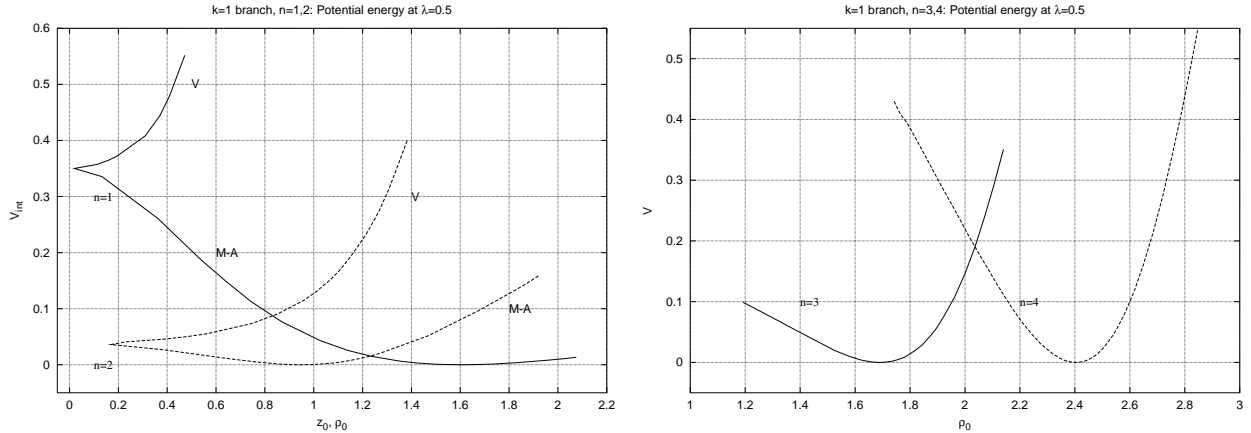


Figure 7: Potential energy of the static solutions of the $k = 1$ branch at $\lambda = 0.5$.

as external magnetic field becomes stronger. The relative distance between the rings also a bit decreases as external field is increasing.

As external magnetic field is directed along positive direction of the z -axis, the external poles are moving away from each other while the location of the inner nodes moves continuously inward, thus the inner M-A pair is squeezing down. There are some indications that for a very large value of the scalar coupling this pair merges into a vortex ring.

Recall that structure of the nodes of the Higgs field for the solutions with $n \geq 3$ on that branch is already different: the modulus of the Higgs field vanishes in two planes parallel to the xy -plane which are centered around the z axis [10]. For this double vortex ring solutions, we observe a completely analogous pattern as for the single vortex on the branch $k = 1$: an external electromagnetic interaction allows us to manipulate the radius of these rings in a similar way.

For the $k = 3$ branch, we observe the same general pattern again. The chain solutions ($n \leq 2$) consist of 3 monopole-antimonopole pairs and for each pair the dependence of the location of nodes on the external field reproduces the picture above. The same pattern holds for vortex solutions: for the triple vortex ring solutions on that branch ($n \geq 3$) each vortex ring evolves as a single vortex solution on the branch $k = 1$.

IV. CONCLUSIONS

We have shown, that the complicated structure of the short-range Yukawa interactions whose balance yields the static axially symmetric non-BPS solutions of the $SU(2)$ Yang-Mills-Higgs model, may be modelled by an effective potential of the electromagnetic interaction between the poles. For a given axially symmetrical Ansatz there is a local minimum of such a potential of interaction. The structure of the electromagnetic interaction in such a system may be investigated as the configuration becomes coupled with an external weak homogeneous magnetic field. The latter is used as a perturbation parameter. This perturbation allows us to reveal a monopole-vortex transition that is observed at some critical value of the magnitude of the external field.

One may conjecture that such a potential of monopole-antimonopole interaction may result, for example, in appearance of an intermediate long-living breather state in the process of annihilation of the configuration into the trivial vacuum. Study of this process will be presented elsewhere.

We believe that the general axially-symmetric Ansatz (2) may also describe two separated monopoles, which are aligned in the isospace. Then it may be possible to provide a similar picture of an effective electromagnetic interaction between the monopoles as well. By making use of the simple electromagnetic analogy one may conjecture that there is a current ring associated with each monopole. However such a static solution may exist in the BPS limit only.

Acknowledgments

I am grateful to B. Kleihaus, J. Kunz and P. Sutcliffe for useful discussions and comments. I would like to acknowledge the hospitality at the Bogoliubov Laboratory of Theoretical Physics, JINR where this work was completed.

[1] N.S. Manton and P.M. Sutcliffe, *Topological Solitons* (Cambridge University Press 2004)

[2] Ya.M. Shnir, *Magnetic Monopoles* (Springer, Berlin Heidelberg New York 2005)

[3] G. 't Hooft, Nucl. Phys. B **79**, 276 (1974);
A.M. Polyakov, Pis'ma JETP **20**, 430 (1974).

[4] E.J. Weinberg and A.H. Guth, Phys. Rev. D **14**, 1660 (1976).

[5] C. Rebbi and P. Rossi, Phys. Rev. D **22**, 2010 (1980).

[6] R.S. Ward, Comm. Math. Phys. **79**, 317 (1981);
P. Forgacs, Z. Horvath and L. Palla, Phys. Lett. B **99**, 232 (1981);
M.K. Prasad, Comm. Math. Phys. **80**, 137 (1981);
M.K. Prasad and P. Rossi, Phys. Rev. D **24**, 2182 (1981).

[7] see e.g. P.M. Sutcliffe, Int. J. Mod. Phys. A **12**, 4663 (1997);
C. J. Houghton, N. S. Manton and P. M. Sutcliffe, Nucl. Phys. B **510**, 507 (1998).

[8] Bernhard Rüber, Thesis, University of Bonn 1985.

[9] B. Kleihaus and J. Kunz, Phys. Rev. D **61**, 025003 (2000).

[10] B. Kleihaus, J. Kunz and Ya. Shnir, Phys. Lett. B **570**, 237 (2003);
B. Kleihaus, J. Kunz and Ya. Shnir, Phys. Rev. D **68**, 101701 (2003);
B. Kleihaus, J. Kunz and Ya. Shnir, Phys. Rev. D **70**, 065010 (2004).

[11] B. Julia and A. Zee, Phys. Rev. D **11**, 2227 (1975).

[12] E.J. Weinberg, Phys. Rev. D **20** 936 (1979).

[13] B. Hartmann, B. Kleihaus, and J. Kunz, Mod. Phys. Lett. A **15**, 1003 (2000);
B. Kleihaus, J. Kunz and Ulrike Neemann, arXiv: gr-qc/0507047.

[14] E.B. Bogomol'nyi, Yad. Fiz. **24**, 861 (1976);
M.K. Prasad and C.M. Sommerfeld, Phys. Rev. Lett. **35**, 760 (1975).

[15] B. Kleihaus, J. Kunz and D.H. Tchrakian, Mod. Phys. Lett. A **13** 2523 (1998).

[16] C.H. Taubes, Commun. Math. Phys. **97**, 473 (1985); ibid **86**, 257 (1982); ibid **86**, 299 (1982).

[17] N.S. Manton, Nucl. Phys. B **126**, 525 (1977).

[18] V.G. Kiselev and Ya. Shnir, Phys. Rev. D **57**, 5174 (1998);
Ya. Shnir, Mod. Phys. Lett. A **19**, 287 (2004).

[19] B. Kleihaus and J. Kunz, Phys. Rev. Lett. **85**, 2430 (2000).

[20] B. Kleihaus, J. Kunz, and Ya. Shnir, Phys. Rev. D **71**, (2005) 024013.

[21] V. Paturyan, and D.H. Tchrakian, J. Math. Phys. **45**, 302 (2004).

[22] P. Goddard and D. Olive, Rep. Prog. Phys. **41**, 1357 (1978).

[23] N.S. Manton, Nucl. Phys. **B135**, 319 (1978).

[24] M. Hindmarsh and M. James, Phys. Rev. D **49**, 6109 (1994).

[25] W. Schönauer, and R. Weiß, J. Comput. Appl. Math. **27**, 279 (1989);
M. Schauder, R. Weiß, and W. Schönauer, The CADSOL Program Package, Universität Karlsruhe, Interner Bericht Nr. 46/92 (1992).

[26] In earliest study of the axially symmetric configurations, we worked in the gauge where the scalar field components on the spacial asymptotic do not depend on the polar angle [9, 10].